Solvent Effect on the Isomerization Rate of Calix[4]arene Studied by Molecular Dynamics Simulations

W. K. den Otter and W. J. Briels*

Contribution from the Chemical Physics Laboratory, University of Twente, P.O. Box 217, 7500 AE Enschede, The Netherlands

Received December 9, 1997. Revised Manuscript Received August 17, 1998

Abstract: The isomerization rates of a calix[4]arene in benzene and in chloroform have been calculated by using molecular dynamics simulations. The reaction coordinate that is employed is based on the unstable normal mode at the saddle point of the potential energy surface. The free energy as a function of this coordinate has been calculated by means of umbrella sampling. Comparison of the free energies in the solvents with those in vacuum reveals that both solvents destabilize the paco conformation and stabilize the transition state region. In chloroform the calix[4]arene shows a stronger preference for the cone conformation than in benzene or in vacuum. The isomerization rate has been determined by the reactive flux method. In benzene the transmission coefficient is about a third higher than in chloroform. The calculated rates are in perfect agreement with experimental data.

I. Introduction

Calix[4]arenes, cyclic arrays of four phenol rings, are versatile molecules:[1] they are used as building blocks in supramolecular chemistry, they can selectively bind ions, they show nonlinear optical behavior, and they can take on various conformations. The latter property will be studied in this paper. In the "cone" conformation all phenol rings are orientated in the same direction, see Figure 1. The molecule is then stabilized by four internal hydrogen bonds at the lower rim of the molecule. In the partial cone conformation, "paco" for short, one of the phenol rings is rotated with respect to the other three phenol rings, see Figure 1. During the isomerization from cone to paco the methylene groups between the phenol rings act as the hinges around which the phenol ring rotates, and the hydroxyl moiety moves through the central annulus.[2] The paco conformation has only two internal hydrogen bonds, making it energetically less stable than the cone conformation by about 10 kcal/mol. The energy barrier between the two conformations is about 15 kcal/mol,[3,4] so the isomerization rate is of the order of 100 s^{-1} at 300 K. This energy barrier makes it impossible to calculate the isomerization rate by simply monitoring the conformation of the molecule during a long molecular dynamics simulation (MD).[5] Currently simulations up to a dozen nanoseconds are feasible, but the isomerization reaction requires a simulation of the order of a second long to produce a reliable result. In this contribution we apply statistical mechanical theories which make it possible to calculate very slow reaction rates by simulations of only a few nanoseconds.

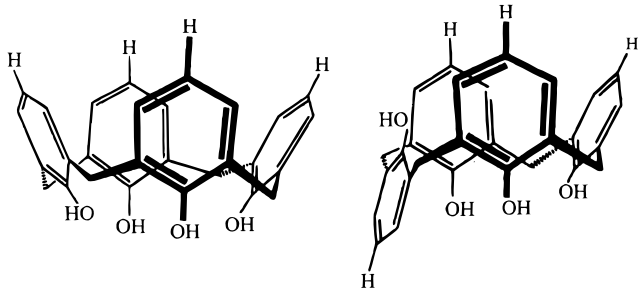

Figure 1. Cone (left) and paco (right) conformations of a calix[4]-arene.

In Section II we will see that reaction rates are conveniently expressed as products of two factors. The first factor, the transition state theory rate, depends on the free energy difference between the reactant well and the transition state.[6] Several methods are available nowadays for calculating relative free energies as a function of the conformation of a reacting molecule. These methods and a wide variety of applications are covered by several reviews.[7−11] The second factor, the transmission coefficient,[6] corrects for so-called recrossings, which are ignored in transition state theory, and at the same time makes the reaction rate independent of the somewhat arbitrary definition of the transition state. This coefficient has been calculated for a number of isomerization reactions, as well as for a few chemical reactions.[12,13] A third important quantity

(1) (a) Gutsche, C. D. *Calixarenes*; Royal Society of Chemistry: Cambridge, U.K. 1989. (b) Vicens, J. D.; Böhmer, V., Eds. *Calixarenes. A Versatile Class of Compounds*; Kluwer Academic Publishers: Dordrecht, The Netherlands, 1991.

(2) Fischer, S.; Grootenhuis, P. D. J.; Groenen, L. C.; van Hoorn, W. P.; van Veggel, F. C. J. M.; Reinhoudt, D. N.; Karplus, M. *J. Am. Chem. Soc.* **1995**, *117*, 1611−1620.

(3) Gutsche, C. D.; Bauer, L. J. *J. Am. Chem. Soc.* **1985**, *107*, 6052−6059.

(4) Araki, K.; Shinkai, S.; Matsuda, T. *Chem. Lett.* **1989**, *1989*, 581−584.

(5) Frenkel, D.; Smit, B. *Understanding Molecular Simulation*; Academic Press: San Diego, CA, 1996; pp 176−178, 249−260.

(6) Hänggi, P.; Talkner, P.; Borkovec, M. *Rev. Mod. Phys.* **1990**, *62*, 251−341.

(7) Jorgensen, W. L. *J. Phys. Chem.* **1983**, *87*, 5304−5314.

(8) Beveridge, D. L.; DiCapua, F. M. *Annu. Rev. Biophys. Biophys. Chem.* **1989**, *18*, 431−492.

(9) Brooks, C. L., III; Case, D. A. *Chem. Rev.* **1993**, *93*, 2487−2502.

(10) van Gunsteren, W. F.; Beutler, T. C.; Fraternali, F.; King, P. M.; Mark, A. E.; Smith, P. E. In *Computer Simulations of Biomolecular Systems*; van Gunsteren, W. L., Weiner, P. K., Wilkinson, A. J., Eds.; ESCOM: Leiden, The Netherlands, 1993; Vol. 2, pp 315−348.

(11) Straatsma, T. P. *Rev. Comp. Chem.* **1996**, *9*, 81−127.

10.1021/ja9741739 CCC: $15.00
Published on Web 12/08/1998

in reaction rate theory is the reaction coordinate.[6] We have recently introduced a convenient definition of this coordinate, based on the unstable normal mode at the saddle point of the potential energy surface.[14,15] This definition is computationally efficient, and can be applied to a wide variety of reactions.

Conformations of calix[4]arenes[2,16] and of numerous derivatized calix[4]arenes have been studied in a series of molecular mechanics studies in vacuum, using various force fields.[2,16−20] In the case of the calix[4]arene, all calculations agree on the order of stability of the four possible conformations, but they do not agree on the energies of these conformations, nor on the symmetry of the cone conformation. Wipff, Varnek, and coworkers[21,22] published a series of articles on simulations of derivatized calix[4]arenes in several solvents, concentrating on the complexation with neutral guests and cations. For uncomplexed calix[4]crown6 the conformation calculated to be the most stable in vacuum differed from the most abundant conformation observed experimentally in chloroform, indicative of significant conformation dependent solvation energies.[22] Recently, van Hoorn *et al*.[17] explained in a qualitative way the discrepancy between the conformational distributions in vacuum and in two solvents of two derivatized calix[4]arenes. Among the properties of calix[4]arenes that have extensively been measured are the isomerization rates in solvents. These rates were found to strongly depend on the lower rim substituant, and to a lesser extent on the solvent and the upper rim substituant.[3,4,16,17] Calculations in vacuum, especially of minimum energies and saddle point energies,[2,19] may yield a reasonably good estimate of the reaction rate, but, of course, they cannot account for the solvent effect. Grootenhuis *et al.*,[18] performing simulations of calix[4]arenes in water, observed several transitions within 50 ps, but these astonishingly high rates cannot be confirmed experimentally since calix[4]arene does not dissolve in water.

Simulations with an explicit solvent model offer valuable insights into the effect of the solvent on the equilibrium constant and on the reaction rate.[7−13,23] In some isomerization reactions the solvent effect is prominent, as for proteins[8,9] and for molecules that are capable of including a solvent molecule,[17] while in other cases it is of minor importance. In this contribution we present calculations of the cone−paco equilibrium distribution and isomerization rate in two different solvents, and compare the results with experiments.

II. Theory

II.A. Reaction Rate. The forward reaction rate is defined as the fraction of reactants that turns into products per unit of time.[6] We shall assume that the rate is predominantly determined by the (free) energy barrier separating reactants from products. To calculate the reaction rate, we first of all need a method of telling reactants and products apart. We therefore introduce the reaction coordinate,[6,24,25] ξ, which is taken to be a function of the coordinates of the reacting molecule only. The reaction coordinate is defined in such a way that it is larger than $\xi^\ddagger$ for products and smaller than $\xi^\ddagger$ for reactants. Conformations with $\xi = \xi^\ddagger$ are at the dividing plane between reactants and products, the so-called transition state, which is located in the sparsely populated area at the top of the energy barrier. The definition of the reaction coordinate employed in this article is deferred until the next section.

In Eyring's transition state theory (TST) the rate is expressed as the instantaneous product bound flux through the transition state, normalized by the number of reactant molecules:[6,25,26]

$$k^{\mathrm{TST}}{}_{\mathrm{f}} = \frac{\langle|\dot{\xi}|\rangle_{\xi^\ddagger}}{2} \frac{P(\xi^\ddagger)}{\int_{-\infty}^{\xi^\ddagger} P(\xi)\,\mathrm{d}\xi} \qquad \text{(II.1)}$$

where $\dot{\xi} = \mathrm{d}\xi/\mathrm{d}t$. The first factor on the right-hand side is half the average absolute velocity of molecules at the transition state; the half arises because only half the molecules crossing the transition state have a positive velocity, i.e. are going from the reactant state to the product state. Once the definition of the reaction coordinate is chosen, this factor is readily evaluated.[6] In the second factor we have used the probability distribution of the reaction coordinate in the canonical ensemble,[5]

$$P(\xi) = \frac{1}{Q} h^{-3N} \int\int \delta[\xi(\mathbf{X}) - \xi] \exp[-\beta H(\mathbf{X},\mathbf{p}_X)]\,\mathrm{d}\mathbf{X}\,\mathrm{d}\mathbf{p}_X \qquad \text{(II.2)}$$

where H is the Hamiltonian, $\mathbf{X}$ is the collection of all $3N$ coordinates of the reacting molecule and the solvent, $\mathbf{p}_X$ are the conjugate momenta, δ is the Dirac delta function, h is Planck's constant, and $\beta = 1/k_B T$ with T the absolute temperature and k_B Boltzmann's constant. The partition function Q arises as the normalization factor of the distribution. The second factor in eq II.1 is therefore to be interpreted as the probability for a molecule in the reactant state to reach the transition state. Two methods for calculating the probability distribution are discussed in Section II.C.

It is a well-known fact that transition state theory overestimates the true reaction rate.[6,24−26] The underlying reason simply is the implicit assumption of TST that each molecule crossing the transition state with a positive velocity will end up in the

(12) Whitnell, R. M.; Wilson, K. R. *Rev. Comp. Chem.* **1993**, *IV*, 67−148.
(13) Anderson, J. B. *Adv. Chem. Phys.* **1995**, *XCI*, 381−431.
(14) den Otter, W. K.; Briels, W. J. *J. Chem. Phys.* **1997**, *106*, 5494−5508.
(15) den Otter, W. K.; Briels, W. J. *J. Chem. Phys.* **1997**, *107*, 4968−4978.
(16) (a) Harada, T.; Rudzinski, M.; Osawa, E.; Shinkai, S. *Tetrahedron* **1993**, *49*, 5941−5954. (b) Harada, T.; Ohseto, F.; Shinkai, S. *Tetrahedron* **1994**, *50*, 13377−13394. (c) Harada, T.; Shinkai, S. *J. Chem. Soc., Perkin Trans. 2* **1995**, 2231−2242.
(17) van Hoorn, W. P.; Briels, W. J.; van Duynhoven, J. P. M.; van Veggel, F. C. J. M.; Reinhoudt, D. N. *J. Org. Chem.* **1998**, *63*, 1299−1308.
(18) Grootenhuis, P. D. J.; Kollman, P. A.; Groenen, L. C.; Reinhoudt, D. N.; van Hummel, G. J.; Ugozzoli, F.; Andreetti, G. D. *J. Am. Chem. Soc.* **1990**, *112*, 4165−4176.
(19) (a) Royer, J.; Bayard, F.; Decoret, C. *J. Chim. Phys.* **1990**, *87*, 1695−1700. (b) Thondorf, I.; Brenn, J.; Brandt, W.; Böhmer, V. *Tetrahedron Lett.* **1995**, *36*, 6665−6668. (c) van Hoorn, W. P.; Morshuis, M. G. H.; van Veggel, F. C. J. M.; Reinhoudt, D. N. *J. Phys. Chem. A* **1998**, *102*, 1130−1138.
(20) (a) Lipkowitz, K. B.; Pearl, G. *J. Org. Chem.* **1993**, *58*, 6729−6736. (b) Harada, T.; Rudzinski, J. M.; Shinkai, S. *J. Chem. Soc. Perkin Trans. 2* **1992**, 2109−2115. (c) Dickert, F. L.; Schuster, O. *Adv. Mater.* **1993**, *5*, 826−829.
(21) (a) Guilbaud, P.; Varnek, A.; Wipff, G. *J. Am. Chem. Soc.* **1993**, *115*, 8298−8312. (b) Varnek, A.; Wipff, G. *J. Phys. Chem.* **1993**, *97*, 10840−10848. (c) Wipff, G.; Engler, E.; Guilbaud, P.; Lauterbach, M.; Troxler, L.; Varnek, A. *New J. Chem.* **1996**, *20*, 403−417. (d) Fraternali, F.; Wipff, G. *J. Incl. Phenom. Mol. Recog. Chem.* **1997**, *28*, 63−78.
(22) Wipff, G.; Lauterbach, M. *Supramol. Chem.* **1995**, *6*, 187−207.
(23) (a) Duffy, E. M.; Severance, D. L.; Jorgensen, W. L. *J. Am. Chem. Soc.* **1992**, *114*, 7535−7542. (b) Blake, J. F.; Lim, D.; Jorgensen, W. L. *J. Org. Chem.* **1994**, *59*, 803−805. (c) Lim, D.; Hrovat, D. A.; Thatcher Borden, W.; Jorgensen, W. L. *J. Am. Chem. Soc.* **1994**, *116*, 3494−3499. (d) Evanseck, J. D.; Houk, K. N.; Briggs, J. M.; Jorgensen, W. L. *J. Am. Chem. Soc.* **1994**, *116*, 10630−10638. (e) Lim, D.; Jorgensen, W. L. *J. Am. Chem. Soc.* **1996**, *100*, 17490−17500.
(24) Atkins, P. W. *Physical Chemistry*; Oxford University Press: Oxford, U.K., 1990; pp 484−492, 597−600, 840−869.
(25) Chandler, D. *J. Chem. Phys.* **1978**, *68*, 2959−2970.
(26) Eyring, H. *J. Chem. Phys.* **1935**, *3*, 107−115.

product well. However, chances exist that a molecule crossing the transition state with a positive velocity rapidly recrosses the transition state before settling in the product well, e.g. after colliding with a solvent molecule. Likewise, a molecule crossing the transition state with a negative velocity can recross the transition state with a positive velocity to return to the product state. Both these cases contribute to the TST rate, but neither of them corresponds to a reaction, as the molecule returns to its initial state. In textbooks this fact is compensated for ad hoc by multiplying the TST rate with a transmission coefficient, κ, whose value lies between zero and one:[24]

$$k_f = \kappa k_f^{TST} \tag{II.3}$$

It is less well-known that the transmission coefficient can be calculated exactly, under the condition that classical mechanics adequately describes the motion of the molecule. From Onsager's regression hypothesis it follows that[6,25]

$$\kappa = \kappa(t), \qquad t_{recross} < t < 1/k_f \tag{II.4}$$

$$\kappa(t) = \frac{\langle \delta[\xi(0) - \xi^{\ddagger}]\dot{\xi}(0)\theta[\xi(t) - \xi^{\ddagger}]\rangle}{\langle \delta[\xi(0) - \xi^{\ddagger}]\dot{\xi}(0)\theta[\dot{\xi}(0)]\rangle} \tag{II.5}$$

where θ is the Heaviside step function, t and 0 denote the time, and the broken brackes indicate a canonical average. The denominator of eq II.5 is the average velocity of molecules crossing the transition state at time 0 in the positive direction, i.e. the first factor on the right-hand side of eq II.1. The numerator is the average velocity of molecules crossing the transition state at time 0 of those molecules that are in the product state some time t after crossing the transition state, regardless of the initial crossing direction. One readily sees that in the limit of t going to zero the numerator equals the denominator. At longer times the contributions of recrossing trajectories will start to diminish the transmission coefficient (it may temporarily increase, though, depending on the characteristics of the reaction). After some time, which is longer than the typical time of the molecular motions but much shorter than the time constant of the reaction, the transmission coefficient will stabilize at some plateau level,[6,25] eq II.4. At this point all molecules which crossed the transition state at time 0 have reached either the product well or the reactant well, and will stay there for a long while until they incidentally escape. The numerator of eq II.5 then contains contributions only from those molecules that originated in the reactant well and have settled in the product well, hence the name reactive flux method[6] (RF). By inserting the plateau value of the transmission coefficient into eq II.3 we find the exact rate. Note that the transmission coefficient is easily calculated by MD simulations:[5] first one samples configurations in the dividing plane, and next one calculates relaxation runs to see where each of these configurations ends up about a picosecond later.

From eq II.1 it follows that the TST rate constant depends on the precise definition of the dividing plane between reactants and products. Obviously, the dividing plane must lie near the top of the energy barrier to cohere with the intuitive notion of reactants and products. But there is no clear reason why one plane in this region should be preferred over another, or to put it differently, why one TST rate is better than another. The only thing one knows for sure is that even the lowest TST rate still is an upper limit to the true rate (since $\kappa \leq 1$). It has been shown that the reactive flux method does not suffer from these problems: provided the dividing plane lies near the top of the barrier, the reactive flux method will always yield the same rate constant.[5,25,27] The only problem is that the number of relaxation runs required to accurately calculate the transmission coefficient increases exponentially as the plateau value of the transmission coefficient decreases. We therefore now set forth to find a reaction coordinate that yields a high plateau value, i.e. a low TST rate.

II.B. Reaction Coordinate. A particularly important point on the potential energy surface of the reacting system is the saddle point, the lowest point on the top of the energy barrier: any molecule going from the reactant state to the product state must at least rise to the energy of the saddle point to overcome the reaction barrier.[24] According to the Boltzmann distribution, molecules crossing the barrier will do so preferably with the least amount of energy, so the majority of the molecules will surmount the barrier in the vicinity of the saddle point. It is only natural, therefore, to introduce a reaction coordinate based on the properties of the saddle point, as will be done next.

Suppose we have located the first-order saddle point, $\mathbf{R}^0$, of the potential energy surface of an N atom molecule. For notational convenience and to make the results more transparent, we have collected all $3N$ coordinates into a single mass-weighted column vector, $\mathbf{R}^0 = (\sqrt{m_1}(\mathbf{r}_1^0)^T, ..., \sqrt{m_N}(\mathbf{r}_N^0)^T)^T$, where $\mathbf{r}_i^0$ is the column vector of the coordinates of atom i with mass m_i. We shall assume that there is no external potential acting on the molecule. At the saddle point the gradient of the potential energy is zero, so a Taylor expansion up to second order of the potential energy yields an energy of

$$\Phi(\mathbf{X}) = \Phi(\mathbf{R}^0) + {}^1/_2(\mathbf{X} - \mathbf{R}^0)^T\,\mathbf{H}(\mathbf{X} - \mathbf{R}^0) \tag{II.6}$$

at a point $\mathbf{X}$ close to the saddle point. The Hessian matrix, $\mathbf{H}$, contains all second derivatives of the potential energy with respect to the mass-weighted Cartesian coordinates. This matrix is then diagonalized to find its eigenvectors and eigenvalues, just as one normally does for a molecule at the potentiel energy minimum.[24]

The eigenvectors of the Hessian can be subdivided into two groups. The first group contains the three eigenvectors $\mathbf{E}^k$ which correspond to a rigid body translation and the three eigenvectors $\mathbf{S}^k$ which correspond to a rigid body rotation. In the absence of an external field, one easily sees that the potential energy of the molecule does not change during these moves, hence the eigenvalues of these six eigenvectors are all equal to zero. The second group contains the $3N - 6$ eigenvectors with a nonzero eigenvalue, the normal modes of vibration.[24] These vibrations are, in first order approximation, independent of one another; the eigenvalues are the squares of the frequencies of vibration, which are experimentally accessible. If the Hessian were to be evaluated at a local minimum of the potential energy surface, then all eigenvalues would be positive: move along any normal mode, starting from $\mathbf{R}^0$, and the potential energy will rise. At a first-order saddle point, however, there is exactly one eigenvector with a negative eigenvalue, i.e. an imaginary eigenfrequency. Move along this direction, henceforth called the unstable normal mode $\mathbf{Q}^r$, and the potential energy will fall. In other words, in this direction the molecule is going from the saddle point toward the product (or reacant) well. As an illustration of this unstable normal mode, the resulting atomic displacements of a calix[4]arene at the cone to paco saddle point are depicted in Figure 2.

(27) Miller, W. H. *Acc. Chem. Res.* **1976**, *9*, 306−312.

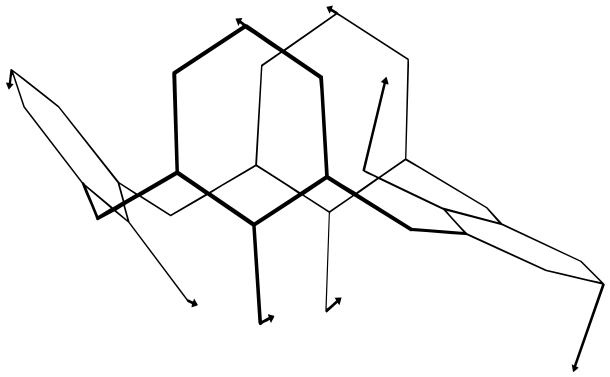

Figure 2. Saddle point configuration of a calix[4]arene. The arrows attached to the atoms indicate how the atoms move under the unstable normal mode $\mathbf{Q}^r$.

We now define the reaction coordinate as the displacement of the molecule, with respect to the saddle point, along the unstable direction. For a molecule with coordinates $\mathbf{X}$ we thus arrive at the projection

$$\xi = \frac{(\mathbf{X} - \mathbf{R}^0)\cdot\mathbf{Q}^r}{\mathbf{Q}^r\cdot\mathbf{Q}^r} \tag{II.7}$$

The particularly simple form of this equation arises because the eigenvectors of the Hessian are orthogonal. Conventional TST calculations[6,26] in which the rate is obtained from the positive eigenfrequencies at the energy minimum and the saddle point are in fact based on this definition of the reaction coordinate.

At this point the reader might argue that the above definition of the reaction coordinate is intuitively appealing, but that under simulation conditions the definition is useless since it is not invariant under rotations. To solve this problem we exploit the freedom in choosing the saddle point configuration: the rotated saddle point, $\mathbf{AR}^0 = (\sqrt{m_1}(\mathbf{ar}_1^0)^T, \ldots, \sqrt{m_N}(\mathbf{ar}_N^0)^T)^T$, where $\mathbf{a}$ is an ordinary three-dimensional rotation matrix, is also a saddle point. One readily verifies that the eigenvectors of the Hessian are rotated in the same manner, so the unstable normal mode of the rotated saddle point is $\mathbf{AQ}^r$. By inserting these two rotated vectors into eq II.7, the reaction coordinate becomes a function of the coordinates $\mathbf{X}$ and the rotation matrix $\mathbf{a}$,

$$\xi = \frac{(\mathbf{X} - \mathbf{AR}^0)\cdot\mathbf{AQ}^r}{\mathbf{Q}^r\cdot\mathbf{Q}^r} \tag{II.8}$$

We now must find a connection between $\mathbf{X}$, $\mathbf{R}^0$, and $\mathbf{a}$ to make the definition of the rotation matrix, and hence the definition of the reaction coordinate, unequivocal. Analogous to eq II.8, we may calculate the "rotation" of the molecule with respect to $\mathbf{AR}^0$ as the projection of the displacement $\mathbf{X} - \mathbf{AR}^0$ onto the $\mathbf{AS}^k$, the three rotated rotational eigenvectors of the Hessian. The correct rotation matrix $\mathbf{a}$ is then defined as the one that makes all three projections simultaneously equal to zero. A more elaborate discussion of this topic, and an algorithm to calculate the rotation matrix are given elsewhere.[14]

II.C. Free Energy. It is common practice to convert probability distributions and partition functions, as defined by eq II.2, into free energies,

$$A(\xi) = -k_B T \ln P(\xi) + c \tag{II.9}$$

where c is an irrelevant constant arising from the partition function Q. The RF rate then reads[15]

$$k_f = \kappa\sqrt{\frac{k_B T}{2\pi}}\langle|\nabla_x\xi|\rangle_{\xi^\ddagger}\, e^{-[A(\xi^\ddagger)-A_R]/k_B T} \tag{II.10}$$

where we have combined eq II.1 through II.3. Here A_R is the free energy of the reactant well, obtained by replacing $P(\xi)$ in eq II.9 by the denominator of the second factor in eq II.1. With the reaction coordinate as defined in Section II.B we find $|\nabla_x\xi| = 1\ \mathrm{kg}^{-1/2}\ \mathrm{m}^{-1}$ at the saddle point, and this value increases only slightly on taking the average over the saddle plane. In the experimental literature a slightly different definition of the free energy is commonly used, by writing a measured reaction rate as

$$k_f = \frac{k_B T}{h}\, e^{-\Delta A^\ddagger/k_B T} \tag{II.11}$$

By comparing the two above expressions we find

$$\Delta A^\ddagger = A(\xi^\ddagger) - k_B T \ln\left[\sqrt{\frac{h^2}{2\pi k_B T}}\langle|\nabla_x\xi|\rangle_{\xi^\ddagger}\right] - A_R - k_B T \ln\kappa \tag{II.12}$$

The second term on the right-hand side removes from $A(\xi^\ddagger)$ the contribution of the velocity $\dot{\xi}$, so the free energy difference $\Delta A^\ddagger$ is based on the probability of finding a molecule at the transition state with zero crossing velocity, while the free energy $A(\xi^\ddagger)$ is based on the probability for the molecule to be at the transition state regardless of the crossing velocity. Notice that $\Delta A^\ddagger$ also includes a contribution from the transmission coefficient, while $A(\xi^\ddagger)$ does not.

Perhaps the best known method of calculating the free energy of a molecule *in vacuo*, i.e. A_R, is to perform a normal mode analysis.[24] Contributions from the $3N - 6$ eigenfrequencies of vibration, the inertia tensor, and the total mass of the molecule give the desired result. The assumptions underlying this theory are that the amplitudes of the vibrations are small, and that there is no coupling between rotations and vibrations. As we have shown elsewhere,[15] it is straightforward to calculate the free energy as a function of the reaction coordinate under the same conditions. The basic task is to calculate the lowest energy conformation and the $3N - 7$ eigenfrequencies of vibrations in the hyperplane of configurations with a prescribed value of the reaction coordinate. The method is reliable and fast for calculations *in vacuo*, but it is of little practice for a molecule in a solvent, since the inclusion of solvent effects in the theory is virtually impossible.

An alternative method for calculating the free energy would be to directly sample the probability distribution of the reaction coordinate of the solvated molecule in a long simulation. Obviously, the height of the energy barrier between reactants and products would create insurmountable difficulties. The barrier region would be sampled very poorly, and the molecule might even stay in one conformation for the entire run. In fact, this is precisely the problem that we try to avoid by using reaction rate theory. Suppose now that we add to the existing potential energy surface a so-called umbrella potential,[5,28] $U(\mathbf{X})$. The probability distribution of the system with the umbrella reads as

(28) (a) Kumar, S.; Bouzida, D.; Swendsen, R. H.; Kollman, P. A.; Rosenberg, J. M. *J. Comput. Chem.* **1992**, *13*, 1011−1021. (b) Bartels, C.; Karplus, M. *J. Comput. Chem.* **1997**, *18*, 1450−1462.

$$P_U(\xi) = \frac{1}{Q_U} h^{-3N} \int\int \delta[\xi(\mathbf{X}) - \xi] \exp[-\beta\{H(\mathbf{X},\mathbf{p}_X) + U(\mathbf{X})\}] \, d\mathbf{X} \, d\mathbf{p}_X \quad \text{(II.13)}$$

In case the umbrella is a function of the reaction coordinate only, the unbiased distribution may be calculated according to

$$P(\xi) = cP_U(\xi)e^{\beta U(\xi)} \quad \text{(II.14)}$$

where c is a proportionality constant. The probability distribution of ξ in the biased run is thus seen to be easily converted into the probability distribution of the unbiased run. This holds true regardless of the umbrella potential used, so we are free to choose the umbrella that suits us the best. The best choice is $U(\xi) = -A(\xi)$, since it renders P_U independent of ξ. In the biased run the barrier between reactants and products then effectively vanishes, and both configurations can be sampled efficiently with a single long simulation. In such a simulation the reaction coordinate behaves like a diffusing particle. An obvious problem is that we do not know $A(\xi)$ in advance, but by making a good initial guess, as in the above discussed normal mode method, we can get close enough for the method to work properly. If the long simulation samples the entire range of the reaction coordinate but the distribution is not reasonably flat, then the sampled distribution P_U may be converted into a potential by means of eq II.9, and this potential may then be added to the existing umbrella to define a new trial umbrella for a second simulation. Alternatively, we may choose the umbrella in such a way that only a small range of ξ, a so-called window, is sampled. Combining the probability distributions P from different windows by making them match in the region where the windows overlap one another then yields the desired result. Techniques for automated improvement of the umbrella by using all previous simulations are available.[28]

III. Results

The calix[4]arene was modeled with the all-atom CHARMM parameter set 22.[2] The saddle points on the potential energy surface of a calix[4]arene *in vacuo* were calculated by using the conjugate peak refinement algorithm[2,29] implemented in QUANTA/CHARMM.[30] All other calculations were done with GROMOS87,[31] which we adapted to meet our specific needs. The saddle points were transported to GROMOS87, and then further refined by using full-dimensional Newton−Raphson to minimize the length of the gradient of the potential down to 1.8×10^{-10} kcal mol^{-1} Å^{-1}. All normal modes were calculated, and their eigenfrequencies were found to be almost identical to the frequencies obtained by QUANTA/CHARMM after a similar refinement. The positive value of the reaction coordinate for the cone to paco transformation was chosen to correspond to the paco conformation. In all calculations the relative dielectric constant ϵ_r was set equal to one, and no cut-off radius was used for nonbonded interactions.

III.A. Free Energy. The minimum energy conformations as a function of the reaction coordinate for the molecule *in vacuo* were calculated by using Newton−Raphson in which only the reaction coordinate was kept at a prescribed value. In most cases the projection of the gradient onto the plane of constant ξ, i.e. the part of the gradient that is minimized under the constraint on ξ, reached 10^{-9} kcal mol^{-1} Å^{-1}. For each conformation a constrained normal mode analysis was performed to calculate the free energy as a function of the reaction coordinate at 300 K. Both the minimum energy and the free energy functions are plotted in Figure 3. From the latter function follows a free energy difference between the paco well and the cone well of 7.9 kcal/mol. The free energy difference between the saddle plane and the cone well, $A(0) - A_{cone} = 13.1$ kcal/mol, results in the rate $k_f^{TST} = 174$ s^{-1}.

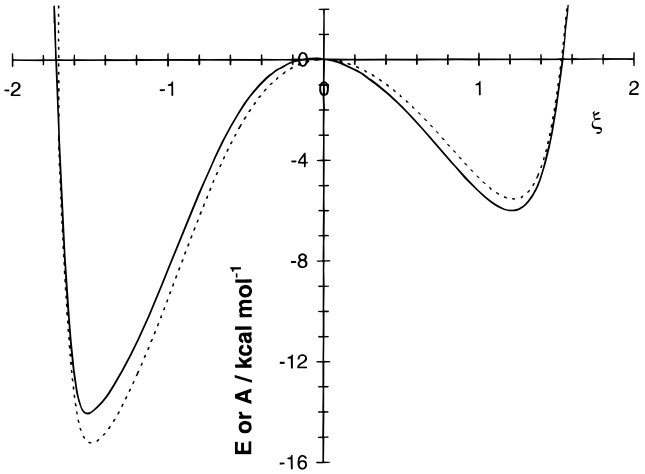

Figure 3. Minimum energy (dotted) and free energy as calculated by means of umbrella sampling (solid) as a function of the reaction coordinate for a calix[4]arene *in vacuo*.

The free energy function obtained by the normal mode analysis was used as the umbrella potential in a vacuum simulation. Since the free energy curve is rather steep at the outermost values of the range of the reaction coordinate, and since it is a little noisy in these regions because of problems with the minimization procedure, we decided to smooth the umbrella by replacing it with a fit. Previously we noticed that small deviations in the fit were very much reflected in the probability distribution P_U. Therefore, the free energy function was fitted with two 15th-order polynomials, one for the cone well and the saddle point region, and one for the paco well and the saddle point region. In the saddle point region a third-order polynomial was used to make a smooth transition from one fit to the other. The motion of the reaction coordinate was limited to the region between roughly −1.8 and +1.6 to prevent the molecule from sampling highly improbable conformations, and to reduce the chances of "spontaneous" conformational transitions due to the high stress in the molecule at these extremes. This was done by adding two Fermi−Dirac-like functions to the umbrella, chosen such that they were virtually zero in the region of interest and rapidly increased at the borders. During the simulation the lengths of the bonds involving a hydrogen atom were constrained by using SHAKE.[32] Langevin dynamics[33] with a friction constant of 1 ps^{-1} was used to maintain a temperature of 300 K, to promote the energy exchange between vibrational modes, and to make the molecule rotate with a variable angular momentum. The simulation lasted 30 ns, with a time step of 2 fs. The probability distribution of the biased run was very flat, see Figure 4, indicating that the normal mode based free energy is an excellent approximation of the real free energy. Inserting the distribution and the umbrella in eq II.14, we find $A(0) - A_{cone} = 12.9$ kcal/mol and $k_f^{TST} = 241$ s^{-1}.

(29) Fischer, S.; Karplus, M. *Chem. Phys. Lett.* **1992**, *194*, 252−261.
(30) Brooks, B. R.; Bruccoleri, R. E.; Olafson, B. D.; States, D. J.; Swaminathan, S.; Karplus, M. *J. Comp. Chem.* **1983**, *4*, 187−217.
(31) Berendsen, H. J. C.; van Gunsteren, W. F. *GROMOS Reference Manual*; University of Groningen: Groningen, The Netherlands, 1987.
(32) Ryckaert, J.-P.; Ciccotti, G.; Berendsen, H. J. C. *J. Comput. Phys.* **1977**, *23*, 327−341.
(33) Allen, M. P.; Tildesley, D. J. *Computer Simulation of Liquids*; Oxford Science Publications: Oxford, UK, 1987; pp 152−155, 259−260.

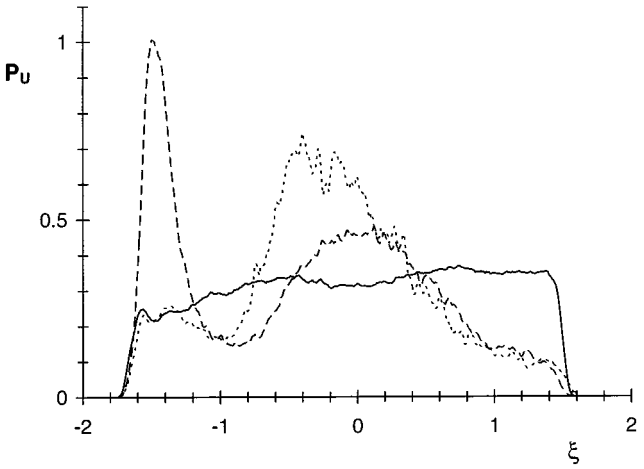

Figure 4. Probability distributions P_U *in vacuo* (solid), choroform (dashed), and benzene (dotted), all corresponding to the same umbrella. The areas under the curves are equal.

During the simulation we encountered the problem that molecules in the $\xi \approx 0.5$ region occasionally made transitions from a paco conformation to a "1,2-alternate" conformation. In this conformation two neighboring phenol rings are pointing upward and the other two are pointing downward, allowing for two internal hydrogen bonds. Once the molecule reached the 1,2-alternate conformation it never returned to the paco conformation. There are two ways for a paco to transform into a 1,2-alternate, depending on whether the second rotated phenol ring neighbors the first rotated phenol ring on the left or on the right.[15] Both 1,2-alternates have the same energy, but the two paco to 1,2-alternate transition states have slightly different energies because of the orientation of the hydrogen bonds. The reason for the occurrence of the unwanted side reactions was that the umbrella lowered not only the cone to paco transition state but also the two paco to 1,2-alternate transition states. To prevent these rare side reactions we expanded the umbrella by adding two Fermi−Dirac-like potentials, each depending on the reaction coordinate of one of the saddle points of the paco to 1,2-alternate barrier. Equations II.13 and II.14 were adapted accordingly. These added potentials were found to hardly effect the motion of the molecule for most of the time, but they did prevent transitions from a paco to a 1,2-alternate conformation.

To calculate the isomerization rate of a calix[4]arene dissolved in benzene, we first simulated a box of pure benzene. We used the Lennard-Jones parameters and the charges of the rigid benzene model by Jorgensen and co-workers,[34] which were previously used in Monte Carlo[34] and MD[35] simulations. The force field was augmented by adding bonded-interaction terms. Since the nonbonded parameters of the CH groups in benzene are identical with those of the 12 CH groups in the calix[4]arene, we decided to use the relevant bonded parameters of the calix[4]arene for the benzene as well. The cubic simulation box contained 343 molecules. A thermostat[37] kept the temperature at 300 K with a time constant of 0.1 ps. The C−H bond lengths were constrained by using SHAKE.[32] Every tenth simulation step the list of interacting charge groups (=CH) was updated to contain all groups within 13 Å of each other; the interactions between these groups were calculated each time step. At the same time, the interactions of charge groups at a distance between 13 and 16 Å was calculated; since this interaction changes relatively little during 10 steps it was treated as a constant force/energy that was added to the pair-list-based interactions calculated every time step.[33] No long-range corrections were applied. The box was first equilibrated at a constant volume corresponding to the experimental density.[38] Then a manostat[37] was turned on to keep the pressure at 1 atm, using a typical time constant $\tau_p = 0.5$ ps and the experimental value of the isothermal compressibility,[38] $\beta = 9.7 \times 10^{-10}$ Pa^{-1}. Immediately the volume of the box decreased by about 15%. At this new value the volume oscillated with a period of 10 ps. By increasing τ_p to 5.0 ps, in which case our β to τ_p ratio equalled the one used by Müller-Plathe,[35] the box regained its proper density. We conjecture that the manostat failed because of the shape and corresponding potential of the benzene molecule.

After equilibrating the benzene box at 1 atm, the calix[4]arene and the solvent were combined into a single box, a truncated octahedron of about 52 nm^3 containing 343 benzene molecules. This box was thoroughly equilibrated, at constant volume first and at constant pressure next, before the actual production run began. The normal mode based umbrella, which performed so well *in vacuo*, was used as the umbrella of the solvated molecule. The resulting probability distribution, sampled in 0.75 ns of simulation time, is shown in Figure 4. Comparison of this distribution with the one from the simulation in vacuum beautifully reveals the solvent effect: the probability at $\xi \approx -0.4$ increases drastically, while the paco conformation is depleted. To get better statistics, two additional simulations were run with the same umbrella in which the reaction coordinate was limited to sample a single well only. The three distributions were combined into a single one by matching the probabilities in the regions which were covered by two distributions. As a check, this distribution was transformed into a potential by eq II.9, and added to the existing umbrella. With this new umbrella the distribution in the final run was, indeed, satisfactorily flat. The free energy difference between the paco and the cone was calculated to be 8.4 kcal/mol, and the difference between the saddle plane and the cone is 12.5 kcal/mol, from which finally followed $k_f^{TST} = 471$ s^{-1}.

As a comparison, in Figure 4 we have plotted the probability distribution of a calix[4]arene in chloroform. This distribution was calculated previously, using the same techniques as described here, but with a different umbrella.[15] We converted this distribution into the distribution that we would have obtained in chloroform with the current vacuum umbrella, i.e. the one that was also used in benzene. From the plot it follows that both solvents destabilize the paco conformation. The region around the saddle point is stabilized by both solvents, but appreciably more so by benzene than by chloroform. The main difference between the two solvents occurs in the cone region, which is strongly promoted in chloroform but hardly in benzene. The resulting free energy difference between the saddle plane and the cone well in chloroform, 13.6 kcal/mol, therefore is larger than that in benzene, and the rate $k_f^{TST} = 84$ s^{-1} is smaller than in benzene. At 9.1 kcal/mol the free energy difference between cone and paco is also larger.

(34) (a) Jorgensen, W. L.; Severance, D. L. *J. Am. Chem. Soc.* **1990**, *112*, 4768−4774. (b) Jorgensen, W. L.; Laird, E. R.; Nguyen, T. B.; Tirado-Rives, J. *J. Comput. Chem.* **1993**, *14*, 206−215. (c) We used the Lorentz−Berthelot combination rules for the interaction between unlike atoms.

(35) Müller-Plathe, F. *Macromolecules* **1996**, *29*, 4782−4791.

(36) The reaction coordinate was constrained to zero when sampling the transition state, while in the other two simulations the reaction coordinate was not constrained.

(37) Berendsen, H. J. C.; Postma, J. P. M.; van Gunsteren, W. F.; DiNola, A.; Haak, J. R. *J. Chem. Phys.* **1984**, *81*, 3684−3690.

(38) Weast, R. C., Ed. *Handbook of Chemistry and Physics*, 50th ed.; The Chemical Rubber Co.: Cleveland, OH, 1969; pp C-140, F-12.

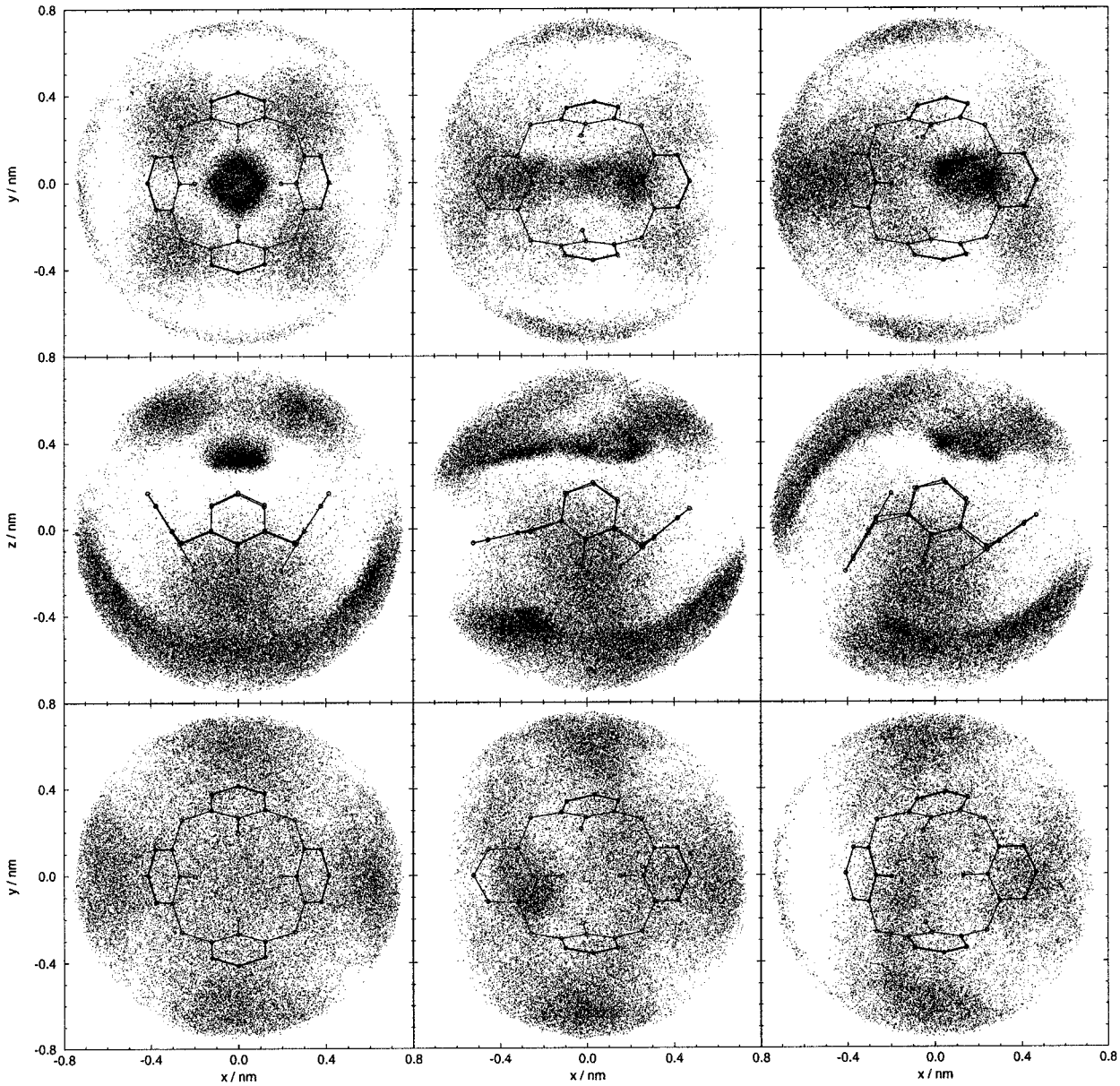

Figure 5. Density distribution of the carbon atom of chloroform, after correction for the orientation of the calix[4]arene. From left to right are shown the cone, transition state, and paco conformation. The middle row gives a side view, the upper row a top view of the carbons with a positive *z*-coordinate, and the bottom row a top view of the carbons with a negative *z*-coordinate. The calix[4]arenes shown are averaged over the simulation.

III.B. Structural Analysis of the First Solvation Shell. From the above results it is clear that the equilibrium distribution and the reaction rate are predominantly determined by the internal energy of the calix[4]arene and to a lesser extent by its interactions with the solvent. It is difficult to determine in which way exactly the interactions between the solute and the solvent, and the induced changes in the entropies and internal energies of the solute and the solvent, affect the reaction.

One way to shed some light on the mutual influence between solute and solvent is by studying the distribution of the solvent in the first solvation shell around the solute. In Figure 5 scatter plots are given of the positions of the chloroform molecules in the first solvation shell around the calix[4]arene molecule. These plots were obtained from simulations of about 2 ns each. During the simulations the calix[4]arene was restricted to sample the cone well, the transition state, and the paco well, respectively.[36] All bonds in which a hydrogen atom takes part were constrained. The solvent molecules were completely rigid. The coordinates of the entire system are saved every 0.1 ps. For the analysis coordinates were translated to the center of mass of the calix[4]arene, and rotated by $\mathbf{a}^{-1}$ where $\mathbf{a}$ is the rotation matrix discussed in Section II.B. The positions of the carbon atoms of all chloroform molecules within 0.75 nm of the origin are plotted in Figure 5. Also plotted are the average positions of the atoms constituting the calix[4]arene.

The plots in the left column of Figure 5 clearly show that the cone configuration captures a chloroform at the upper rim. Note that this chloroform molecule is not inside the cavity, as is observed in *p-tert*-butylcalix[4]arenes complexing with ions and small molecules,[17,21,22] but hovering above the cavity. The captured chloroform molecule is found to constantly move and rotate, with the hydrogen pointing toward the calix[4]arene in one third of the frames, indicating that the dipole of the chloroform molecule has only a minor influence on its orientation. Similarly, at the lower rim the polar hydroxyl groups are not capable of orienting the polar chloroform. Moreover, hardly any structuring of the positions of the chloroform molecules occurs. The plots in the middle column and those in the right

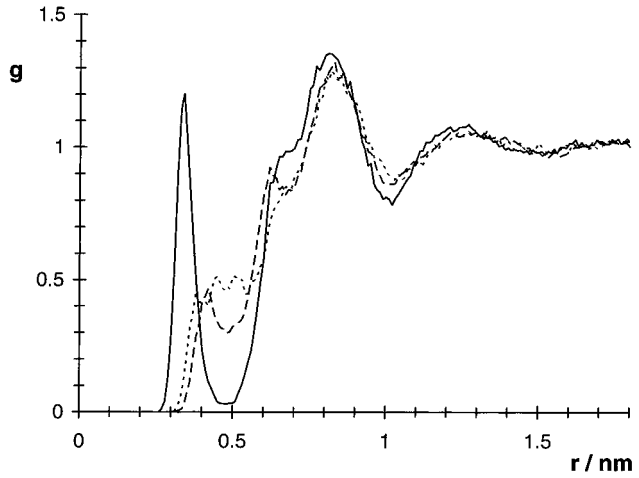

Figure 6. Radial distribution function of the carbon atom of chloroform relative to the center of mass of the calix[4]arene for the cone (solid line), paco (dashed line), and transition state (dotted line) configurations.

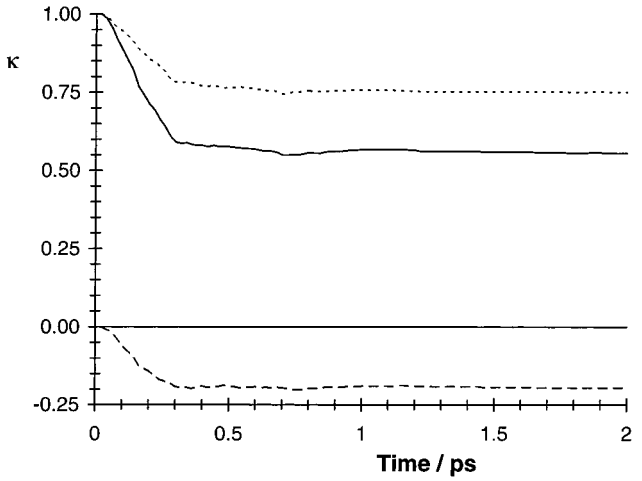

Figure 7. Transmission coefficient (solid) of a calix[4]arene in benzene. The dotted (dashed) line gives the contribution of molecules that settle in the paco conformation after crossing the transition state with a positive (negative) transient velocity.

column show that the transition state and the paco also induce quite some structure in the solvent, but that they do not hold on to a chloroform molecule with the tenacity of the cone conformation. Only the transition state manages to slightly increase the chloroform density at the bottom of the calix[4]-arene, just below the rotating phenol group.

In Figure 6 the radial distribution function of chloroform molecules around the cone, the transition state, and the paco are depicted. In the case of the cone a sharp peak is observed that can be entirely attributed to the captured chloroform at the upper rim. The first minimum in the radial distribution function corresponds to a barrier in the potential of mean force[39] separating the captured molecule from the bulk of the solvent. On average the captured molecule is exchanged with another solvent molecule once every 0.5 ns. From the other two curves in Figure 6 it is obvious that only the paco has a slight tendency to capture a chloroform molecule. To understand why nevertheless the transition state is stabilized by the solvent relative to the paco, we have analyzed the interaction energies of the solvated chloroform molecule with the calix[4]arene. It turned out that these energies have the same minimized value for both configurations, but that the volume corresponding to the minimum interaction energy is much larger for the transition state than for the paco.

Similar simulations to the above have been done with a calix-[4]arene in benzene. The distributions of the centers of mass of the benzene molecule around the calix[4]arene are very similar to those in Figure 5, the main difference being that all maxima and minima are slightly further away from the center of the calix[4]arene due to the size of benzene. Again, the cone conformation captures a benzene molecule. This molecule is standing upright, perpendicular to the annulus of the calix[4]-arene, with a slight preference for the orientation with two CH groups pointing toward the calix[4]arene. In comparison with the chloroform captured at this position, the benzene is relatively weakly bound, while it is exchanged by another benzene roughly once every 0.1 ns. The explanation of the solvent effect in Figure 4 in this case is similar to the above, with the exception that this time the binding interaction between the cone and the captured benzene molecule is much weaker.

III.C. Transmission Coefficient. To calculate the transmission coefficient, eq II.5, conformations needed to be sampled in the transition plane. One thousand conformations were created by means of an MD simulation of a solvated calix[4]arene during which the value of the reaction coordinate was constrained to zero with an algorithm similar to SHAKE;[14] atomic coordinates and velocities were saved every picosecond. Each of these configurations was used as the starting point of a 2 ps relaxation run. At the start of every relaxation run the velocity of the reaction coordinate, which was zero during the constrained run, was replaced by a new velocity drawn from a velocity-weighted Maxwell−Boltzmann distribution.[40] The transmission coefficient as a function of time is shown in Figure 7. The dotted line shows the contribution to the transmission coefficient from those molecules which cross the transition state at time zero with a positive velocity and arrive in the product well, or to put it differently, the fraction of the product bound flux through the transition state that ends up in the product well. Likewise, the dashed line gives the contribution to the transmission coefficient from those molecules which cross the transition state at time zero with a negative velocity and end up in the product state; these molecules must therefore have crossed the transition state at least once. Both curves live up to their expectation: they start at respectively one and zero, at short times they decrease because of molecules recrossing the transition state, and at longer times they settle at a stable level. The solid line, the transmission function, is obtained by summing these two contributions. After 2 ps a plateau of 0.56 is reached. In combination with the previously calculated k_f^{TST}, the true reaction rate is then found to be $k_f^{RF} = 264\ s^{-1}$.

Similar simulations of calix[4]arene in chloroform yielded $\kappa = 0.43$, which together with the transition state value yielded $k_f^{RF} = 36\ s^{-1}$. The influence of the solvent is seen to be more prominent in the free energy differences than on the transmission coefficients.

All results so far have been collected in Table 1, together with a few more results from vacuum simulations. Simulations *in vacuo* with the same transition state produced a transmission coefficient that arrived at a plateau of 0.92 after 0.6 ps, indicating that in this case the TST rate is an excellent approximation of the real rate.[14] After about 0.8 ps the transmission function started to decrease again, and eventually settled at a second

(39) Rey, R.; Hynes, J. T. J. *Phys. Chem.* **1996**, *100*, 5611−5618.

(40) In eq II.5 the velocity of the reaction coordinate ought to be drawn from a Maxwell−Boltzmann distribution, $\exp[-\beta\xi^2]$, but from the equation it follows that it is also possible to draw from the weighted distribution $\xi \exp[-\beta\xi^2]$. The advantage of doing so is that fewer relaxation runs are needed for the averages to converge.

Table 1. Computed and Experimental Rates for the Cone to Paco Conversion

solvent and method	k^{TST}/s^{-1}	κ	k^{RF}/s^{-1}	k^{exp}/s^{-1}
vacuum normal mode analysis	174			
vacuum umbrella sampling, $t = 0.6$ ps	241	0.92	222	
vacuum umbrella sampling, $t = 2.0$ ps	241	0.82	198	
chloroform umbrella sampling	84	0.43	36	30,[a] 8[b]
benzene umbrella sampling	471	0.56	264	202[a]

[a] Data by Gutsche and Bauer,[3] converted to 300 K. [b] Data by Araki *et al.*[4]

plateau of 0.82. This decrease was caused by molecules which left the paco well after having made one full oscillation in this well; this would not have occurred if the paco well had acted as a perfect sink.

The equilibrium conformational distribution and the isomerization rates of calix[4]arenes in solvents have been measured with ^{1}H NMR.[3,4,16,17,41] It was found that for the particular molecule studied here, the paco is too short-lived to be detectable. The measured rate constants therefore correspond to the cone to inverted cone reaction, i.e. a process in which all four phenol rings rotate. This reaction consists of four steps, with one phenol ring rotating in each step.[2] If we assume these steps to be independent, the reaction scheme becomes

$$\mathrm{C} \underset{k_2}{\overset{k_1}{\rightleftharpoons}} \mathrm{P} \underset{k_4}{\overset{k_3}{\rightleftharpoons}} \mathrm{A} \underset{k_3}{\overset{k_4}{\rightleftharpoons}} \mathrm{P}' \underset{k_1}{\overset{k_2}{\rightleftharpoons}} \mathrm{C}' \qquad \text{(III.1)}$$

where C, P, and A denote respectively cone, paco, and alternate, and where primes indicate conformations in which the majority of the phenols are pointing downward. In good approximation the overall cone to inverted cone rate constant is found to be related to the calculated cone to paco rate by[15] $k_{CC'} \approx 3k_f^{RF}$.

Gutsche and Bauer[3] measured the coalescence temperature with temperature-dependent ^{1}H NMR and derived the isomerization rate at this temperature from the chemical shift. They converted the rate into a free energy by

$$\Delta A^{\ddagger} = RT_{\text{coalescence}} \ln\left(\frac{6.62 \times 10^{12}}{k_{\text{coalescence}}}\right) \qquad \text{(III.2)}$$

For calix[4]arene in benzene they found $\Delta A^{\ddagger} = 13.8$ kcal/mol and $T_{\text{coalescence}} = 15$ °C. With these data we have calculated the isomerization rate at the coalescence temperature. By using eq II.11 and assuming that the free energy is independent of the temperature, we then found a rate of 607 s^{-1} at 300 K for the cone to inverted cone reaction, hence a rate of 202 s^{-1} for the cone to paco reaction. The data for a calix[4]arene in chloroform were converted likewise, and yielded a rate of 30 s^{-1}. Araki *et al.*[4] measured the reaction rate and the free energy of a calix[4]arene in chloroform as a function of temperature, resulting in a rate of 8 s^{-1} at 300 K. From their data it followed that the entropic contribution to the free energy is of minor importance in the above extrapolations, at most equal to about 0.1 kcal/mol, which is comparable with the uncertainty of the $\Delta A^{\ddagger}$. All data are summarized in Table 1. The computed reaction rates compare very well with the measured rates, the former being slightly higher.

The agreement of the calculated with the experimental reaction rates adds to the confidence that one may have in the force fields that have been used. Obviously, reaction rates are most sensible to the precise value of $\Delta A^{\ddagger}$. Apparently the present force field has the capability of reproducing a reasonable energy barrier between the cone and paco conformation, and is flexible enough to allow for enough entropy to turn this energy barrier into a good free energy barrier. The fact that two opposite solvent effects with two different solvents are quantitatively reproduced is a remarkable achievement of the force field.

IV. Conclusions

The isomerization rate of a calix[4]arene in benzene and in chloroform has been studied with molecular dynamics simulations. The free energy as a function of the reaction coordinate was calculated by means of umbrella sampling. The rate constants obtained with the reactive flux method were in good agreement with the experimental values. In chloroform the cone conformation was found to be stabilized by the solvent, appreciably reducing the reaction rate with respect to the vacuum value. The reaction coordinate defined as the displacement along the unstable normal mode at the saddle point of the potential energy surface was shown to be very convenient in these calculations. An excellent first guess at the umbrella potential was obtained by a straightforward normal mode analysis. The same reaction coordinate can, in principle, be applied to numerous reactions, including chemical reactions. In the case of an S_N2 reaction, for instance, the harmonic analysis has to be performed on the transition state, including the nucleophile as well as the leaving group.

JA9741739

(41) (a) Happel, G.; Mathiasch, B.; Kämmerer, H. *Makromol. Chem.* **1975**, *176*, 3317−3334. (b) Gutsche, C. D.; Bauer, L. J. *Tetrahedron Lett.* **1981**, *22*, 4763−4766. (c) Groenen, L. C.; van Loon, J.-D.; Verboom, W.; Harkema, S.; Casnati, A.; Ungaro, R.; Pochini, A.; Ugozzoli, F.; Reinhoudt, D. N. *J. Am. Chem. Soc.* **1991**, *113*, 2385−2392. (d) Blixt, J.; Detellier, C. *J. Am. Chem. Soc.* **1994**, *116*, 11957−11960.